

# Detection of Multiple Ophthalmologic Disorders



V.Krishna Sree<sup>1</sup>, P.Sudhakar Rao<sup>2</sup>

<sup>1</sup>Department of ECE

VNR VJIET

<sup>2</sup>Department of ECE, VITS

Hyderabad, India

{sparvatha@gmail.com, kkrishnasree@yahoo.co.in}

**ABSTRACT:** Automated fundus image analysis plays an important role in the computer aided diagnosis of ophthalmologic disorders. A lot of eye disorders, as well as cardiovascular disorders, are known to be related with retinal vasculature changes. Many important eye diseases as well as systemic diseases manifest themselves in the retina. While a number of other anatomical structures contribute to the process of vision, this paper focuses on retinal image analysis and their clinical implications. The most prevalent causes of blindness in the industrialized world are age-related macular degeneration, diabetic retinopathy, and glaucoma. Retinal exudates are among the preliminary signs of diabetic retinopathy, a major cause of vision loss in diabetic patients. Correct and efficient screening of exudates is very expensive in professional time and may cause human error. Nowadays, the digital retinal image is frequently used to follow-up and diagnoses eye diseases. Therefore, the retinal image is crucial and essential for experts to detect exudates. In age related Macular degeneration, the macula is responsible for the sharp central vision needed for detailed activities such as reading, writing, driving, face recognition and ability to see colors. Age related macular degeneration is degeneration of the macula area and the delicate cells of the macula become inactive and stop working. Unfortunately, age-related macular degeneration cannot be completely cured, but if diagnosed at an early stage degeneration laser treatment can help some people to prevent further deterioration of macula. The algorithm locates disease affected pixels on macula and displays their location. After pre-processing particle analysis tool is applied to locate the effected parts on the fundus image.

**Keywords:** Retinal Fundus Image, Glaucoma, Soft Exudates, Hard Exudates, Age Related Macular Degradation and Kirsch Operators

**Received:** 11 October 2013, Revised 18 November 2013, Accepted 26 November 2013

© 2013 DLINE. All Rights Reserved

## 1. Introduction

The eye's fundus is the only part of the human body where the microcirculation can be observed directly. Medical signs that can be detected from observation of eye fundus include hemorrhages, exudates, cotton wool spots, blood vessel abnormalities (tortuosity, pulsation and new vessels) and pigmentation [4] Abnormalities associated with the eye can be divided into two main classes, the first being disease of the eye, such as cataract, conjunctivitis, Blepharitis and glaucoma. The second group is categorized as life style related disease such as hypertension, arteriosclerosis and diabetes.

Ophthalmologists have come to agree that early detection and treatment is the best treatment for this disease. Diabetic mellitus

is a disease caused due to insufficient or nil production of insulin. It develops side effects in organs such as eyes, kidneys, heart and nerves. The effect of diabetes on the eyes is called “*Diabetic retinopathy*”, and it causes many problems to all the parts of the eye and lead to loss of vision finally, if not treated at an earlier stage [2]. Diabetic retinopathy is a degenerative eye disease that occurs in patients with diabetes and is characterized by abnormal blood vessel growth [14]. This can eventually lead to a detached retina and blindness. The disease is classified as Background Diabetic Retinopathy (BDR), Proliferate Diabetic Retinopathy (PDR) and Severe Diabetic Retinopathy (SDR). In BDR stage, the arteries in the retina get weakened and leak forming small dot like hemorrhages. These leaks in blood vessels often lead to swelling or edema in the retina and decreased vision. In the PDR phase, blood circulation is a problem and to acquire sufficient oxygen, new small vessels may grow [9]. This extra blood vessel growth is called ‘*Neovascularisation*’. Blood may leak into the retina and vitreous, causing spots or floaters along with decreased vision. In SDR stage, there is a continuous abnormal vessel growth and scar tissue, which lead to severe damage such as retinal detachment and glaucoma and gradual loss of vision. These Three classes can occur in any of the form either Micro Aneurysms or soft exudates or hard exudates. Micro Aneurysms are the first clinical abnormality to be noticed in the eye [6]. They may appear in isolation or in clusters as tiny, dark red spots or looking like tiny hemorrhages within the light sensitive retina. Their sizes ranges from 10-100 microns i.e. less than 1/12<sup>th</sup> the diameter of an average optics disc and are circular in shape, at this stage, the disease is not eye threatening. Hemorrhages occur in the deeper layers of the retina and are often called ‘*blot*’ hemorrhages because of their round shape. Hard exudates are one of the main characteristics of diabetic retinopathy and can vary in size from tiny specks to large patches with clear edges. As well as blood, fluid that is rich in fat and protein is contained in the eye and this is what leaks out to form the exudates [1]. These can impair vision by preventing light from reaching the retina. Soft exudates are often called ‘*cotton wool spots*’ and are more often seen in advanced retinopathy. Age related macular degeneration [5] begins with characteristic yellow deposits (drusen) in macula. Large and soft drusen are related to elevated cholesterol deposits and may respond to cholesterol lowering agents [3].

In the last years the ophthalmology is always more heavily driven by image analysis. In fact, a number of image analysis tools have been developed for tracing vasculature, identifying key structures, segmenting pathologies and comparing several morphologies to normal ones. In particular, the retinal fundus image analysis allows physicians to detect in more robust and automatic way pathologies as macular degeneration, diabetic retinopathy, glaucoma, retinopathy of prematurity and so on.

Glaucoma is a disease of the major nerve of vision, called the optic nerve. The optic nerve receives light-generated nerve impulses from the retina and transmits these to the brain, where we recognize those electrical signals as vision [10,11]. Glaucoma is characterized by a particular pattern of progressive damage to the optic nerve that generally begins with a subtle loss of side vision (peripheral vision). If glaucoma is not diagnosed and treated, it can progress to loss of central vision and blindness.

Glaucoma is a group of conditions defined by a progressive optic neuropathy with accompanying visual field changes [12]. Glaucoma can be classified as Congenital versus acquired, Open angle versus narrow-angle and Primary versus Secondary. Secondary Glaucoma is of type Pigmentary, Exfoliation, Phacogenic, Phacomorphic, Traumatic, Neovascular and Steroid-induced. Risk Factors for Glaucoma are age, Race (more common in blacks), Family history of glaucoma, Cardiovascular diseases, Myopia, Nutritional factors and migraine. Raised intra-ocular pressure (IOP) is classified as a risk factor but is not part of the definition. When evaluating patients who are suspected glaucoma or to confirm the disease three things need to be monitored. The first and easiest parameter to monitor is intra-ocular pressure and this is done using a form of tonometry. The next parameter to monitor is visual fields. This is carried out in the majority of cases using the Humphrey field analyzer. Glaucoma causes permanent loss of the peripheral field which can be demonstrated by a visual field test [13]. The visual field is very dependent of patient co-operation and concentration. Although the test can take 3-4 minutes it is a very difficult test to do and there can be wide variations in the field from one day to the next. The final parameter to monitor is the optic disc appearance and it does not fluctuate from day to day and unlike fields is not dependent on patient co-operation. It has the potential therefore to be the most useful indicator of disease and disease progression. However, disc evaluation to be of use in glaucomatous patients has to be done with great care and attention to detail [15].

## 2. Materials

In this work, 44 images of STARE database are used for experimentation. Retinal fundus image is the image of the retina obtained by using a special device called fundus camera. It takes the photograph of the interior surface of the eye including the retina, optic disc, macula and posterior pole. The images are captured with 35 ° field of view, and stored in RGB (red, green, blue) color format is given in Figure, image with age related macular degeneration in Figure 2, image with Glaucoma in Figure 3, image with

Hard image with Hard exudates in Figure 4 and image with Soft exudates in Figure 5.

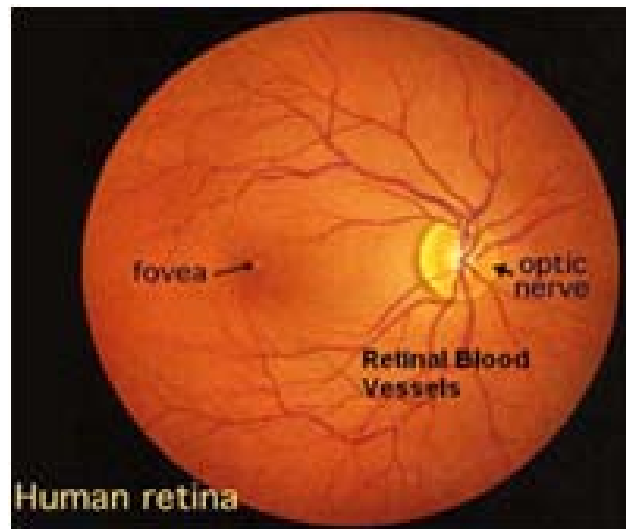


Figure 1. Healthy Retinal fundus image



Figure 2. Image with Age related macular degeneration

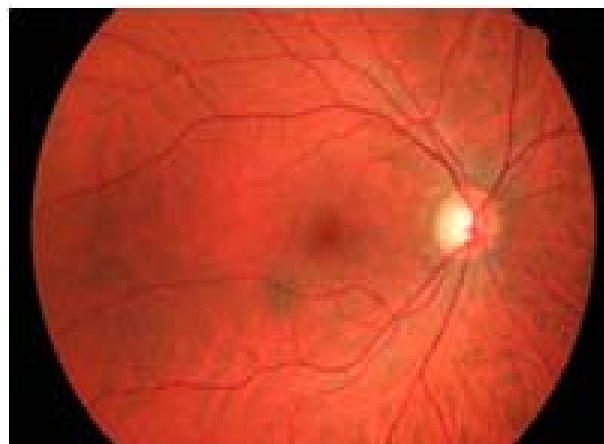


Figure 3. Image with Glaucoma



Figure 4. Image with Hard exudates



Figure 5. Image with Soft exudates

The steps involved for detection of Hard exudates are given in Fig.6. The input image with hard exudates was read, the green component of the image is extracted and the edges were detected. It was followed by averaging and filtering the image using second order Gaussian filter. Adaptive histogram equalization was carried out to enhance the image. The resultant image is now thresholded and processed by the kirsch's operators to remove the blood vessels. Further the remaining noise is removed by median filter.

The input image with soft exudates was read, the green component of the image is taken and the image was adjusted to required intensities. It was followed by obtaining the connected components in the image. Then these connected components were labeled. The areas of the connected components were computed and compared with the threshold value.

The input fundus image with age related macular degeneration was read and the back ground was subtracted from the fundus image. Extract the red and green components from the subtracted image. Adjust the thresholding to the image to extract the drusen part of the image and then convert the image to the black and white format to get the required output.

The input fundus image is read. The green component of the image is considered for examination as it is more suitable for processing. The blood vessels are extracted using improved matched filter which tailor made for the Stare database. The image is split the image into 4 parts, and individual part areas are found. A circular mask is constructed to extract the blood vessels from the opticdisc. The blood vessels in the four quadrants areobtained by rotating a mask image, the size of the ROI image is taken.

The areas of four parts of optic disk are calculated and the ratio of areas of superior side to nasal side is calculated. The ratio is determined and checkedwhether it is less than or greater than one. Detection of glaucoma is done based on ratio. If the ratio is greater than one it is classified as Nonglaucomatous otherwise it is glaucomatous.

### 3. Method

#### 3.1 Kirsch Templates

The operator takes a single kernel mask and rotates it in 45 degree increments through all 8 compass directions: N, NW, W, SW, S, SE, E, and NE [7], [8]. The kernel masks are givenin (1).

$$\begin{aligned}
 N &= \begin{bmatrix} -3 & -3 & 5 \\ -3 & 0 & 5 \\ -3 & -3 & 5 \end{bmatrix} & S &= \begin{bmatrix} 5 & 5 & 5 \\ -3 & 0 & -3 \\ -3 & -3 & -3 \end{bmatrix} & E &= \begin{bmatrix} 5 & 5 & -3 \\ 5 & 0 & -3 \\ -3 & -3 & -3 \end{bmatrix} \\
 SE &= \begin{bmatrix} -3 & -3 & -3 \\ -3 & 0 & -3 \\ 5 & 5 & 5 \end{bmatrix} & SW &= \begin{bmatrix} -3 & -3 & -3 \\ 5 & 0 & -3 \\ 5 & 5 & -3 \end{bmatrix} & W &= \begin{bmatrix} -3 & 5 & 5 \\ -3 & 0 & 5 \\ -3 & -3 & -3 \end{bmatrix}
 \end{aligned}$$

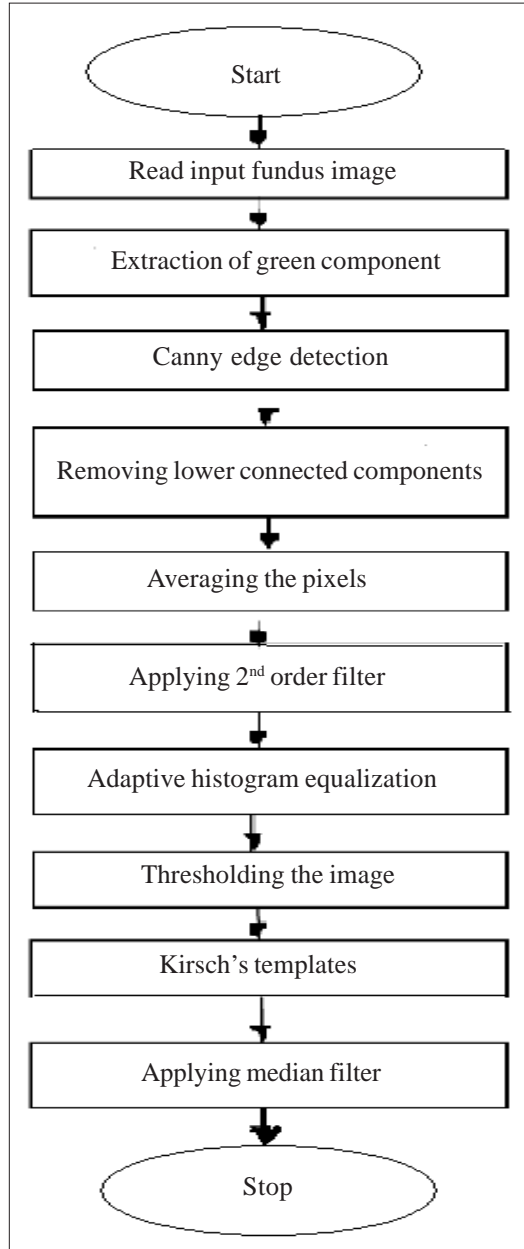


Figure 6. Steps involved for hard exudates detection

$$NW = \begin{bmatrix} 5 & -3 & -3 \\ 5 & 0 & -3 \\ 5 & -3 & -3 \end{bmatrix} \quad NE = \begin{bmatrix} -3 & -3 & 5 \\ -3 & 0 & 5 \\ -3 & 5 & 5 \end{bmatrix} \quad (1)$$

The edge magnitude of the Kirsch operator is calculated as the maximum magnitude across all directions and is given in (2)

$$h_{m,n} = \max_{z=1,8} \sum_{i=-1}^1 \sum_{j=-1}^1 g_{ij} \cdot f_{n+i, m+j} \quad (2)$$

Where  $z$  enumerates the compass direction kernels as

$$g^{(1)} = \begin{bmatrix} 5 & 5 & 5 \\ -3 & 0 & -3 \\ -3 & -3 & -3 \end{bmatrix} \quad g^{(2)} = \begin{bmatrix} 5 & 5 & -3 \\ 5 & 0 & -3 \\ -3 & -3 & -3 \end{bmatrix} \text{ and so on.}$$

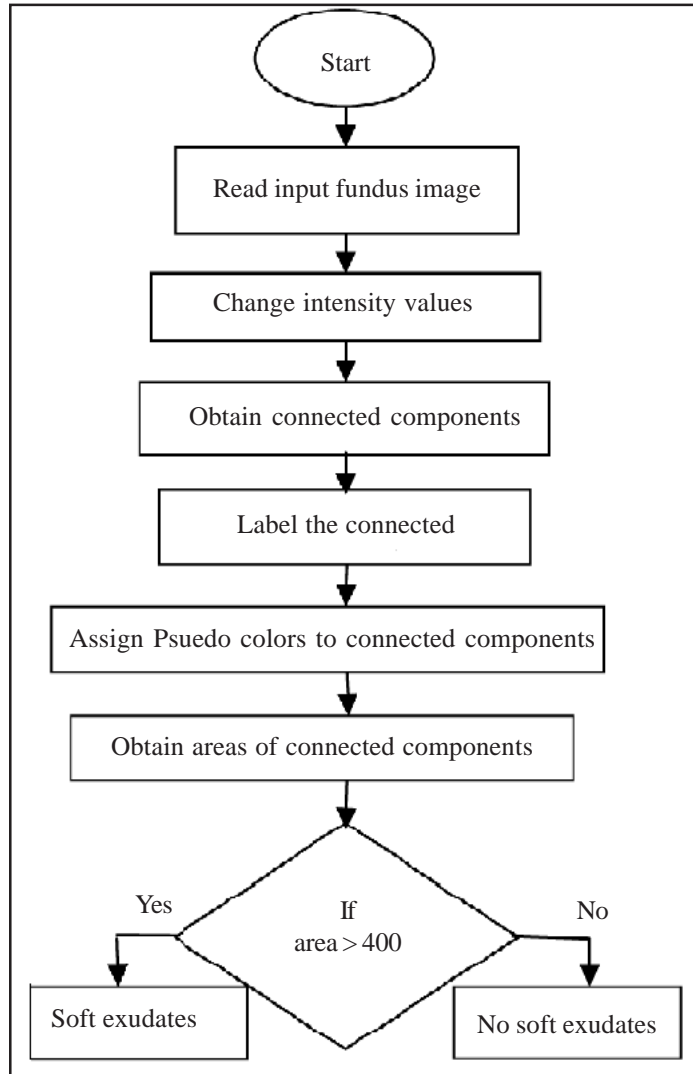


Figure 7. Steps involved for Soft exudates detection

The edge direction is defined by the mask that produces the maximum edge magnitude.

### 3.2 Canny Edge Detection

Edges characterize boundaries and these are areas with strong intensity. The Canny edge detection algorithm is the optimal edge detector with low error rate, well localized and had one response to a single edge. After smoothing the image using a Gaussian mask and eliminating the noise, the edge strength is found by taking the gradient of the image. The Sobel operator performs a 2-D spatial gradient measurement on an image. Then, the approximate absolute gradient magnitude (edge strength) at each point can be found. The Sobel operator uses a pair of  $3 \times 3$  convolution masks, one estimating the gradient in the  $x$ -direction (columns) and the other estimating the gradient in the  $y$ -direction (rows). The magnitude, or edge strength, of the gradient is then approximated using the formula given in (3)

$$|G| = |G_x| + |G_y| \quad (3)$$

Whenever the gradient in the  $x$  direction is equal to zero, the edge direction has to be equal to 90 degrees or 0 degrees, depending on what the value of the gradient in the  $y$ -direction is equal to. If  $G_y$  has a value of zero, the edge direction will equal 0 degrees. Otherwise the edge direction will equal 90 degrees. The formula for finding the edge direction is given in (4).

$$\text{Theta} = \text{Tan}^{-1}(G_y / G_x) \quad (4)$$

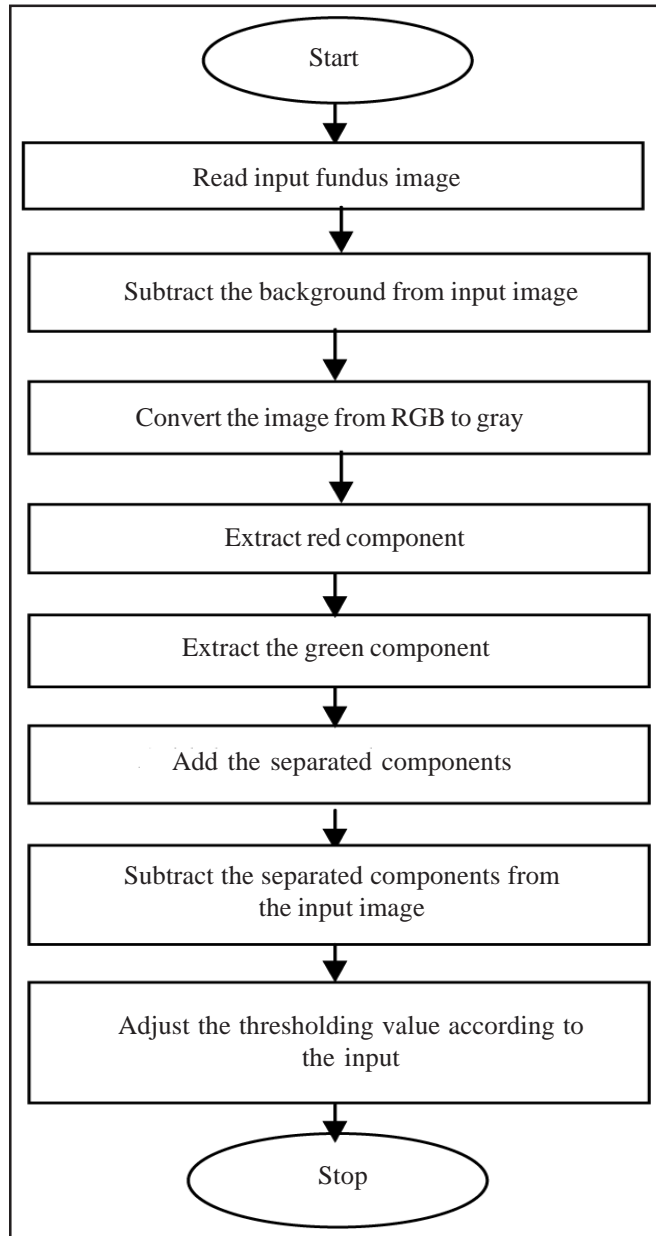


Figure 8. Steps involved for age related macular degeneration detection

### 3.3 Gaussian filtering

The first step in edge detection is to filter out any noise in the original image before trying to locate and detect any edges. And the Gaussian filters which can be computed using a simple mask is used exclusively in the Canny algorithm. Once a suitable mask has been calculated, the Gaussian smoothing can be performed using standard convolution methods. A convolution mask is usually much smaller than the actual image. As a result, the mask is slid over the image, manipulating a square of pixels at a time. The larger the width of the Gaussian mask, the lower is the detector's sensitivity to noise. The localization error in the detected edges also increases slightly as the Gaussian width is increased. At any point  $(x, y)$  in image, the response,  $g(x, y)$  of the filter is the sum of products of the filter coefficients and the image pixels encompassed by the filter is given in (5)

$$g(x, y) = \sum \sum w(s, t) f(x+s, y+t) \quad (5)$$

### 3.4 Connected components and set

A set of pixels in an image which are all *connected* to each other is called a *connected component*. Once region boundaries have

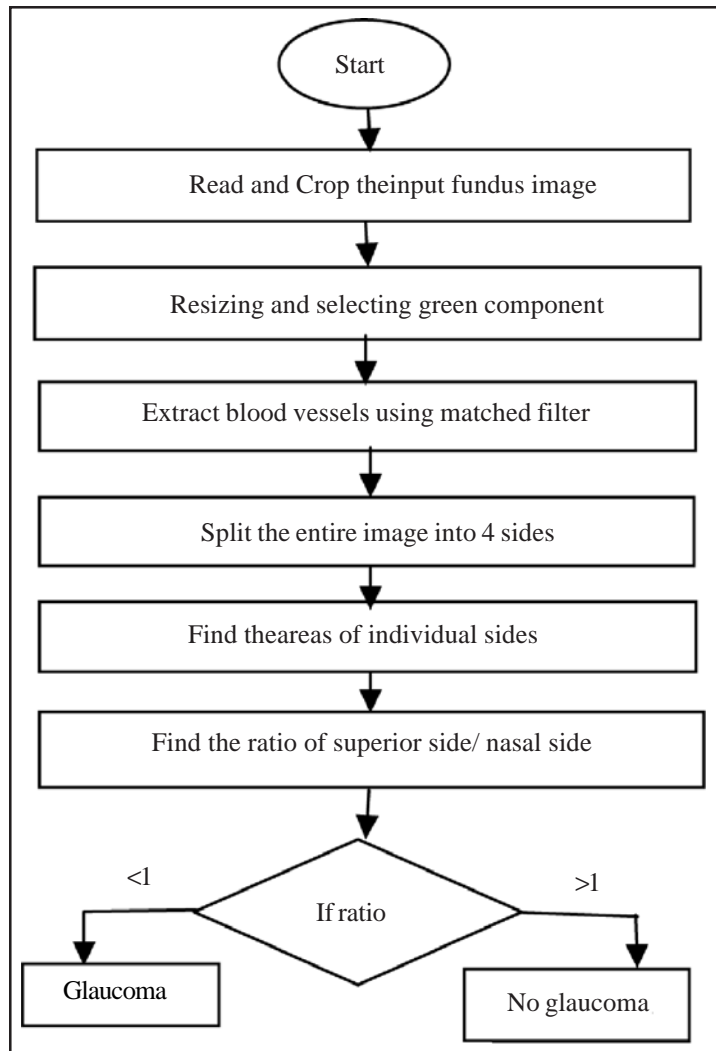


Figure 9. Steps involved in Glaucoma detection

been detected, it is often useful to extract regions which are not separated by a boundary. Any set of pixels which is not separated by a boundary is called connected set. Each maximal region of connected pixels is called a connected component. The set of connected components divides an image into segments.

### 3.5 Connected-component labeling and pseudo coloring

Finding all connected components in an image and marking each of them with a distinctive label is called connected component labeling. A faster-scanning algorithm for connected-region extraction is presented below.

On the first pass iterate through each element of the data by column, then by row. If the element is not the background, get the neighboring elements of the current element. If there are no neighbors, uniquely label the current element and continue, otherwise find the neighbor with the smallest label and assign it to the current element. Store the equivalence between neighboring labels. On the second pass iterate through each element of the data by column, then by row. If the element is not the background re-label the element with the lowest equivalent label. Final result is colored to clearly see two different regions that have been found in the array.

### 3.6 Brightness and Contrast Adjustment



Two commonly used point processes are *multiplication* and *addition* with a constant is given in equation 6

$$g(i, j) = \alpha \cdot f(i, j) + \beta \quad (6)$$

The parameters  $\alpha$  and  $\beta$  are often called the gain and *bias* parameters to control *contrast* and *brightness* respectively. Where  $i$  and  $j$  indicates that the pixel is located in the  $i$ -th row and  $j$ -th column.

### 3.7 Improved Matched Filter

The Extraction of blood vessels is carried by using the improved matched filter. The intensity profile of the blood vessels are approximated by a Gaussian shaped curve given in (7) based on the properties of blood vessels

$$f(x, y) = A \left( 1 - \exp\left(-\frac{u^2}{2\sigma^2}\right) \right) \quad (7)$$

Where  $u$  is the perpendicular distance between the point  $(x, y)$  and the straight line passing through the center of the blood vessel in a direction along its length(y axis) and ' $\sigma$ ' defines the spread of the intensity profile,  $A$  is the gray level intensity of the local background, and  $k$  is a measure of reflection of the blood vessel relative to its neighborhood.  $L$  is the length of the segment for which the vessel is assumed to have a fixed orientation.  $L$  is determined by analyzing vessels in both normal and abnormal retinas. The optimal filter will have the same shape as the intensity profile of blood vessels but the vessels may be oriented at any angle. The matched filter will have its peak response only when it is aligned in the proper direction. Hence the filter is rotated for all possible angles, corresponding responses are compared and for each pixel only the maximum response is retained. To make the response of background with filter to zero, the mean value of kernel is subtracted from the kernel itself. The 2-D matched filter kernel in a discrete grid is designed by using equations from (8) to (13).

Let  $p = [x \ y]$  be a discrete point in the kernel and  $\theta$  be the orientation of the  $i^{\text{th}}$  kernel matched to vessel at angle  $\theta$ . In order to compute the weighting coefficients for the kernel, it is assumed to

$$\bar{r}_i = \begin{bmatrix} \cos\theta_i & -\sin\theta_i \\ \sin\theta_i & \cos\theta_i \end{bmatrix} \quad (8)$$

be centered about the origin  $[0 \ 0]$ . The rotation matrix is given by (8).

And the corresponding point in the rotation co-ordinate system is given by (9).

$$\bar{p}_i = [uv] = pr_i \quad (9)$$

Taking an angular resolution of  $15^\circ$ , 12 different kernels are formed in all possible orientation. A set of 12 such kernels is applied to a fundus image and at each pixel the maximum of their responses is only retained. A Gaussian curve has infinitely long double sided tails and they are restricted to  $\pm 3\sigma$ . A neighborhood  $N$  is defined such that given in (10)

$$N = \{(u, v), |u| \leq 3\sigma, |v| \leq L/2\} \quad (10)$$

The corresponding weights in the  $i$ th kernel are given by (11).

$$K_i(x, y) = \exp\left(-\frac{u^2}{2\sigma^2}\right) \forall p_i \in N \quad (11)$$

And  $\sigma$  is taken as 2.1 after trials to optimize the results. If  $A$  denotes the number of points in  $N$ , the mean value of the kernel is determined as given (12)

$$m = \sum \frac{k_i(x, y)}{A} \quad (12)$$

Thus the convolution mask used in this algorithm is given by (13)

$$K'_i(x, y) = K_i(x, y) - m_i, \forall p_i \in N \quad (13)$$

Because of the hardware design of the image processing system, the weighting coefficients in the kernel need to be in the range

## 2.8. Clinical Assessment of the ISNT Rule for a Normal Optic Nerve

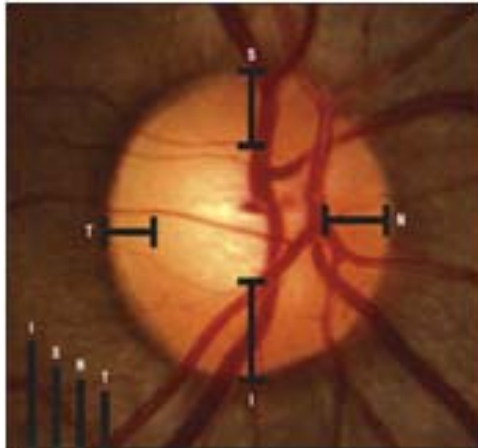


Figure 10. Fundus with ISNT indications

(-128, 127). Hence coefficients are multiplied by a scale factor of 10 and truncated to their nearest integer. Sigma value is used as 2.1 to get optimum results. On the optimum output response image, thresholding is done to extract the blood vasculature.

The ISNT rule is that disc rim thickness shows a characteristic configuration of inferior (*I*) greater than or equal to superior (*S*) greater than or equal to nasal (*N*) greater than or equal to temporal (*T*) (or *I*e”*S*e”*N*e”*T*). The ISNT rule has been used to help diagnose the presence of glaucoma in adults, based on the morphometric characteristics of the optic disc. The normal optic disc usually demonstrates a configuration in which the inferior neuroretinal rim is the widest portion of the rim, followed by the superior rim, and then the nasal rim, with the temporal rim being the narrowest portion. The rule states that, for normal optic discs, the neuroretinal rim width is greatest in the order inferior e” superior e” nasal e” temporal. Glaucoma frequently damages superior and inferior optic nerve fibers before temporal and nasal fibers, leading to thinning of the superior and inferior rims and violation of the rule. Thus, violation of the rule has been shown to have predictive value in diagnosing glaucoma in adults.

## 4. Results and Discussions

The results of Hard exudates are given in Figure 11 (a), (b), (c), (d) (e) and (f). The results of Soft exudates are given in Figure 12 (a), (b), (c) and (d). The results of age related macular degeneration are given in Figure 13 (a), (b), (c), (d) (e) and (f). The results of Glaucoma are given in Figure 14 (a), (b), (c), (d) (e), (f), (g), (h), (i) and (j). The rate of Sensitivity and Specificity are two parameters considered as evaluation parameters and the experimental results are given in Table 1.

### 4.1 iResults of Hard Exudates



Figure 11 (a). Input image

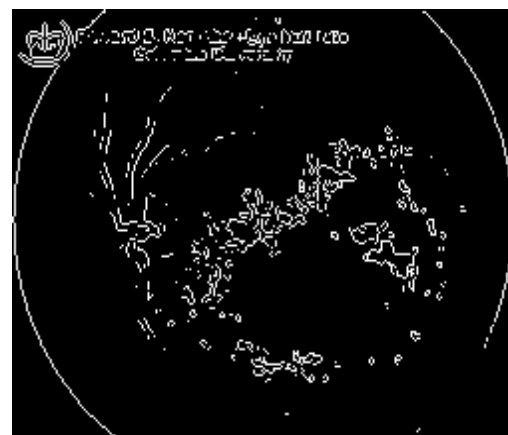


Figure 11 (b). Sobel edge detected image



Figure 11 (c). Image removing some components

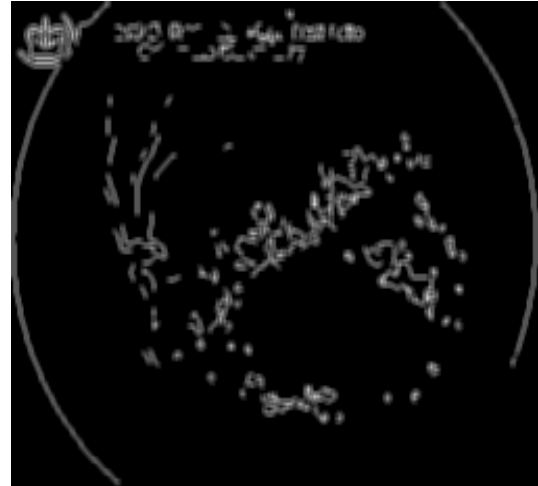


Figure 11 (d) . Average and filtered image

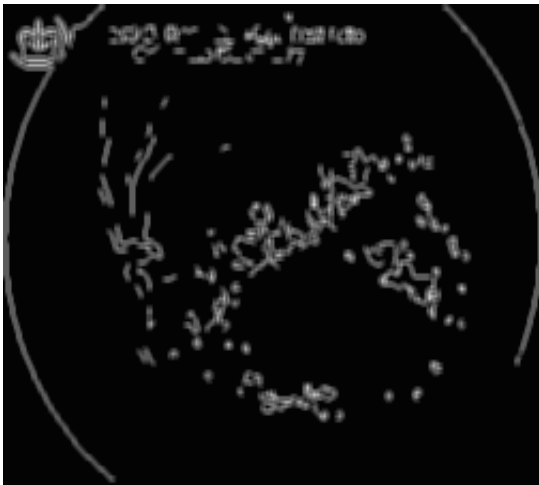


Figure 11 (e). Adaptive histogram equalized image

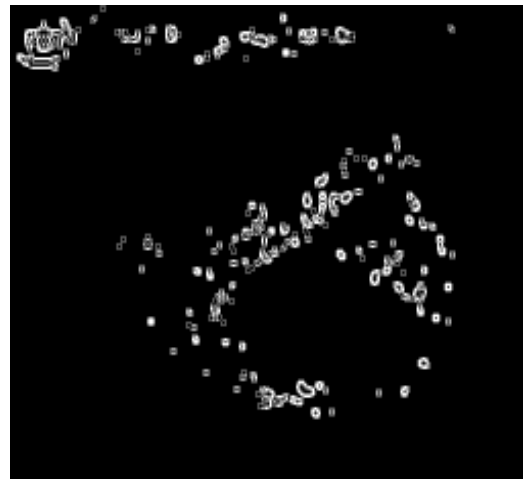


Figure 11 (f). Image after kirsch operation

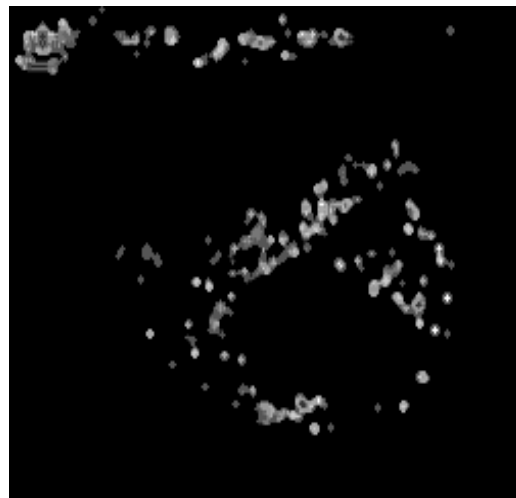


Figure 11 (g). Image after removed noise

#### 4.1 Sensitivity

Sensitivity of a test refers to how many cases of a disease a particular test can find. Numerically sensitivity is the ratio between

#### 4.2 Results for Soft Exudates

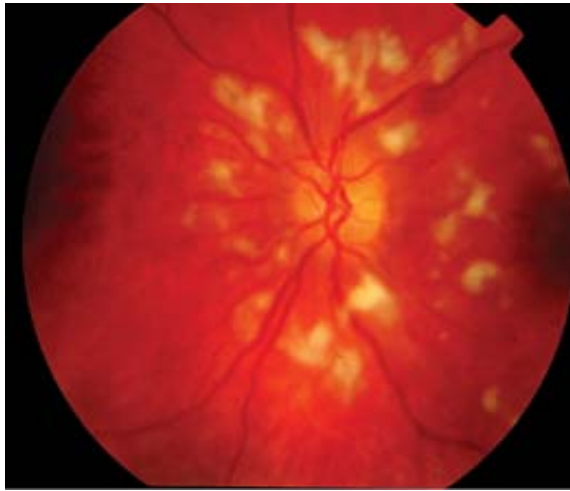


Figure 12 (a). Input image

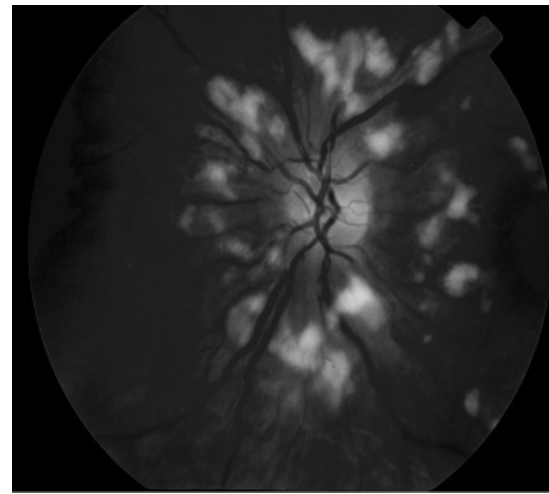


Figure 12 (b). Green component image

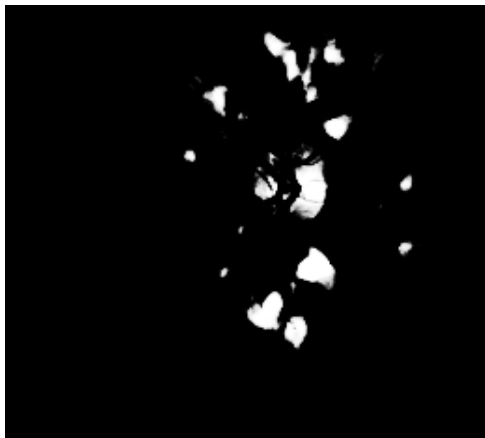


Figure 12 (c). Intensity adjusted image



Figure 12 (d). Random pseudo coloured connected components

#### 4.3 Results For Age Related Macular Degeneration

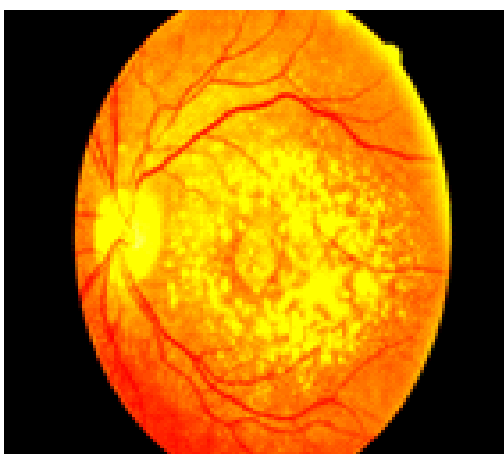


Figure 13 (a). Input image

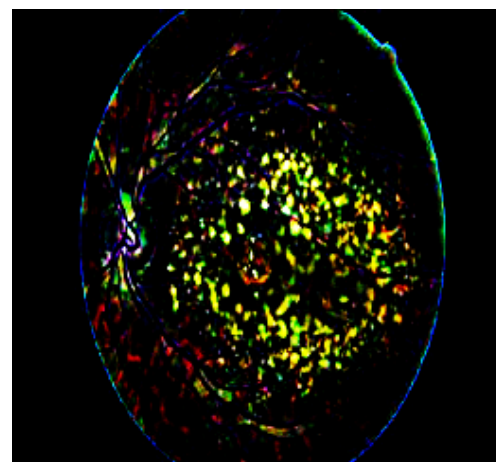


Figure 13 (b). Image after subtracting the input from the background



Figure 13 (c). Image after converting from RGB to gray

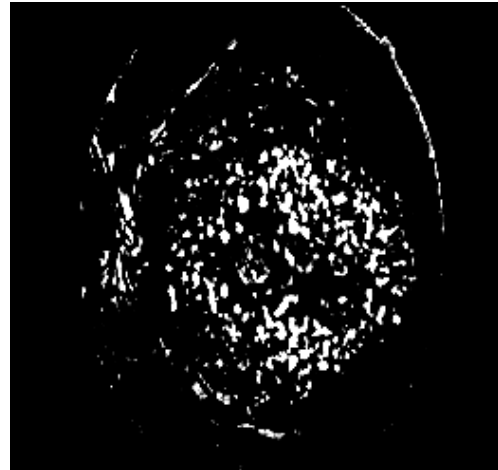


Figure 13 (d). Image with only green components

#### 4.4 Results of Glaucoma

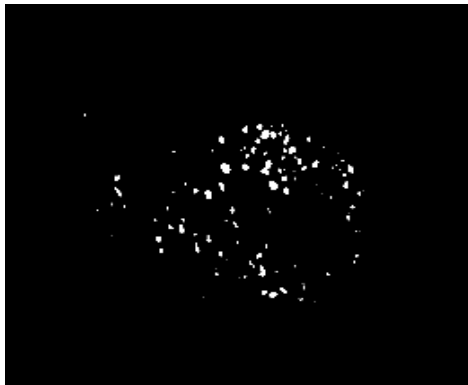


Figure 13 (e). Image after adjusting image intensity values

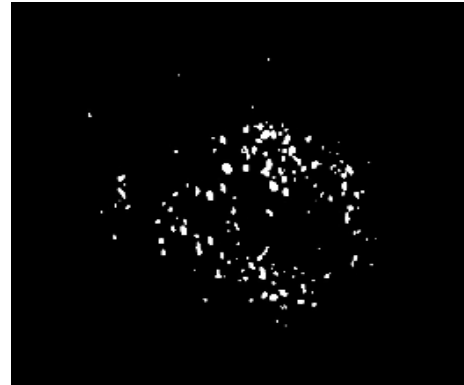


Figure 13 (f). final output

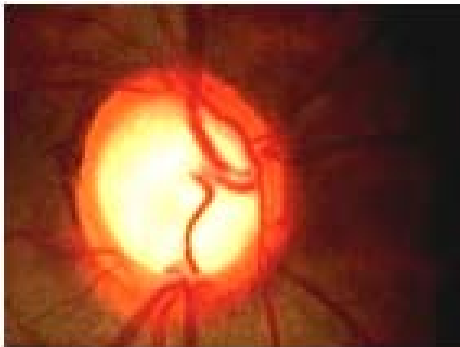


Figure 14 (a). Input image

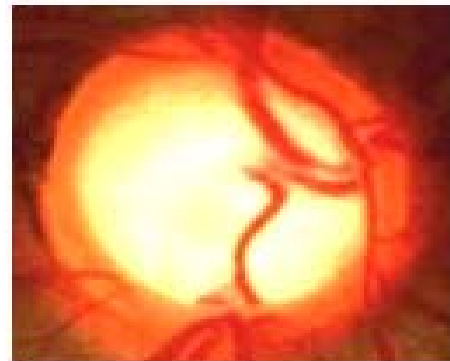


Figure 14 (b). Cropped image

number of true positive (TP) results to the sum of true positive and false negative (FN) results. Sensitivity relates to the test's ability to identify positive results.

$$\text{Sensitivity} = TP / (TP + FN) \quad (14)$$

#### 4.2 Specificity

The specificity of a test refers to how accurately it diagnosed a particular disease without giving false positive results. Numerically, specificity is the ratio between number of true negative results (TN) to the sum of true negative and false positive (FP) results. Specificity relates to the test's ability to identify negative results.



Figure 14 (c). Resized image



Figure 14 (d). Green component

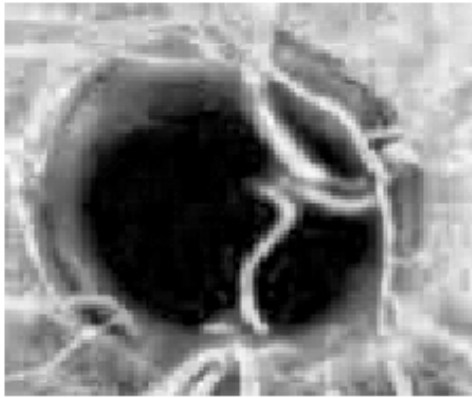


Figure 14 (e). Histogram equalized image



Figure 14 (f). Output of matched filter

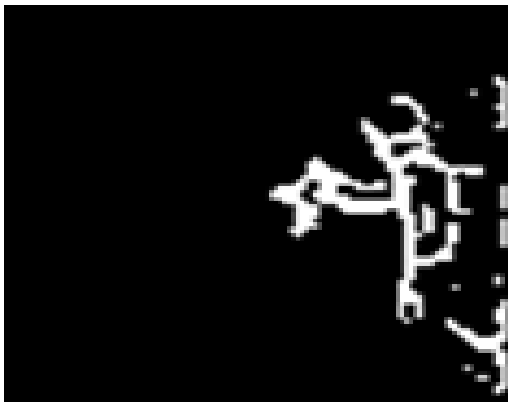


Figure 14 (g). Nasal side



Figure 14 (h). Temporal side

Diseases	Sensitivity	Specificity	Accuracy
hard exudates	0.875	0.333	72.7
Soft exudates	0.775	0.333	66.7
Age related macular degeneration	0.875	0.750	78.9

Table 1. Rate of Sensitivity and Specificity

$$\text{Specificity} = TN / (TN + FP)$$

(15)

#### 4.3 Accuracy

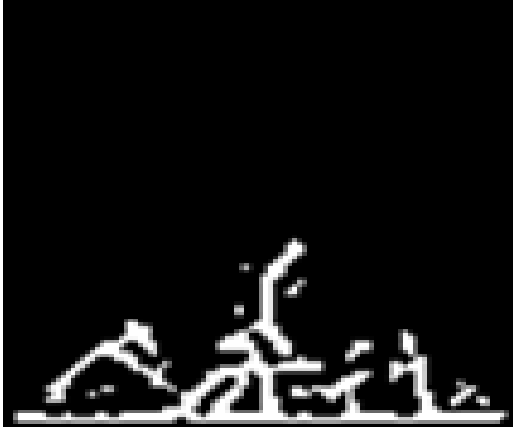


Figure 14 (i). Inferior side



Figure 14 (j). Superior side

Accuracy is defined as the efficiency of classification of fundus images for a particular case

$$\text{Accuracy} = (TP + TN) / (TP + FP + TN + FN) \quad (16)$$

## 5. Conclusion

The feature detection technique applied on retinal fundus images has successfully worked on the images collected from Stare Database. The obtained output images determine the abnormality in an eye. Algorithm has been tested with data set and clinical images. 90% of the images tested and matched with the ground truth. The objective of algorithm is to develop a system which detects hard exudates, soft exudates, and age related macular degeneration automatically. The algorithms were simple, robust and faster. We have tested on total of 44 images out of which 11 were tested on hard exudates and 12 on soft exudates, 4 were tested on Glaucoma and 19 on age related macular degeneration. We obtained sensitivity and specificity as given in table 1, and ISNT ratio as given in table 2.

Normal	Glaucoma
1.3897	0.8455
1.6131	0.7985
1.4020	0.8562
1.0229	0.7122

Table 2. ISNT Ratio

## References

- [1] Sopharak, A., Uyyanonvara, B., Barman, S., Williamson, T. H. (2009). Automatic detection of diabetic retinopathy exudates from non-dilated retinal images using mathematical morphology methods, *In: Computerized Medical Imaging and Graphics*, 32, p. 720–727.
- [2] Kose, C., Sevik, U., Ikibas, C., Erdol, H. (2008). Simple methods for segmentation and measurement of diabetic retinopathy lesions in retinal fundus images, *Computers in Biology and Medicine*, 38, 611 – 619.
- [3] Rapantzikos, K., Zervakis, M., Balas, K. (2003). Detection and segmentation of drusen deposits on human retina: Potential in the diagnosis of age-related macular degeneration, *Medical Image Analysis*, 7, p. 95–108.
- [4] Giancardo, L., Meriaudeau, F., Karnowski, T. P., Li, Y., Garg, S., Tobin Jr, S. W., Chaum, E. (2012). Exudate-Based Diabetic macular edema detection in fundus images using publicly available datasets, *Medical Imaging Analysis*, 16 (1) 216-226.
- [5] Burlina, P., Freund, D. E., Dupas, B., Bressler, N. (2011). Automatic Screening of Age-Related Macular Degeneration and Retinal Abnormalities, *In: Proceedings of 33<sup>rd</sup> Annual International Conference of the IEEE EMBS*, Boston, p. 3962-3966.



- [6] Hipwell, JH., Starchan, F., Olson, JA., McHardy, KC., Sharp, PF., Forrester, JV. (2000). Automated detection of micro aneurysms in digital red-free photographs: A diabetic retinopathy screening tool, *Diabetic Medicine*, Aug, 17 (8) 588-594
- [7] Bahadir karasulu. (2012). Automatic extraction of retinal blood vessels: A soft ware implementation, *European Scientific Journal*, 8 (30) 47-57.
- [8] Bhadauria, H. S., Bisht, S. S., Annapurna singh. (2013). Vessel extraction from retinal fundus images, *IOSR journal of Electronics and communication Engineering*, 6, p. 79-82.
- [9] Chanwimaluang, T., Fan, G. (2003). An Efficient Blood Vessel Detection Algorithm for Retinal Images Using Local Entropy Thresholding, *In: Proceedings of the 2003 International Symposium on Circuits and Systems*, Bangkok, Thailand, 5, p. V-21 - V-24, May.
- [10] Ahmed, W. R., Eswaran, C., Subhas, H. (2009). Automatic tracing of optic disc and exudates from color fundus images using fixed and variable thresholds, *J. Med. Syst.*, 33 (1) 73-80.
- [11] Chrastek, R., M. Wolf and K. Donath. (2005). Automated segmentation of the optic nerve head for diagnosis of glaucoma *Med. Image Anal.*, 9 (4) 297-314
- [12] Kavitha, S., S. Karthikeyan and K. Duraiswamy. (2010). Early detection of glaucoma in retinal images using cup to disc ratio , *IEEE 2<sup>nd</sup> International Conference on Computing, Communication and Networking Technologies*, p. 1-5
- [13] Narasimhan, K., Vijayarekha. (2011). An efficient automated system for glaucoma detection using fundus image, *J. Theoret. Appl. Inform. Techn.*, 33 (1) 104-110.
- [14] Ravishankar, S. J., Mittal, A. (2009). Automated feature extraction for early detection of diabetic retinopathy in fundus images, *IEEE Conference on Computer Vision and Pattern Recognition*, p. 210-217.
- [15] Rajendra, U. A., Sumeet, D., Xian, D. (2011). Automated diagnosis of glaucoma using texture and higher order spectra features, *IEEE Trans. Inf. Technol. Biomed.*, 15 (3) 449-455.